OXFORD UNIVERSITY PRESS | Clinical & Experimental Immunology
The Journal of Translational Immunology

NKG2C+CD57+ natural killer with senescent features cells are induced in cutaneous leishmaniasis and accumulate in patients with lesional healing impairment

Journal:	*Clinical and Experimental Immunology*
Manuscript ID	CEI-2023-10280.R1
Manuscript Type:	Research Article
Date Submitted by the Author:	30-Jan-2024
Complete List of Authors:	Polaco Covre, Luciana; Universidade Federal do Espírito Santo, Núcleo de Doenças Infecciosas; University College London, Medicine Division Fantecelle, Carlos ; Universidade Federal do Espírito Santo, Núcleo de Doenças Infecciosas Queiroz, Ariadne ; UFES Fardin, Julia; UFES Miranda, Pedro Henrique; Universidade Federal do Espírito Santo, Biotecnologia Henson, Sian; QMUL, William Harvey Research Institute Fonseca-Martins, Alessandra Marcia; Universidade Federal do Rio de Janeiro, Instituto de Microbiologia Professor Paulo de Goes de Matos Guedes, Herbert Leonel; Universidade Federal do Rio de Janeiro, Instituto de Microbiologia Professor Paulo de Goes; Fundação Oswaldo Cruz, FIOCRUZ-RJ Mosser, David Michael; University of Maryland College Park, Department of Cell Biology and Molecular Genetics Falqueto, Aloisio; Universidade Federal do Espírito Santo, Medicina Social Akbar, Arne; University College London, Division of Infection and Immunity Gomes, Daniel; Universidade Federal do Espírito Santo, Núcleo de Doenças Infecciosas; University College London, Medicine; Universidade Federal do Espírito Santo, Núcleo de Biotecnologia
Key Words:	Cell Differentiation, Infection, Natural Killer Cells

NKG2C+CD57+ natural killer with senescent features cells are induced in cutaneous leishmaniasis and accumulate in patients with lesional healing impairment

Luciana Polaco Covre[1,2,3#*]; Carlos Henrique Fantecelle[1#]; Ariadne Mendes Queiroz[1], Julia Miranda Fardin[1], Pedro Henrique Miranda[4]; Sian Henson[5]; Alessandra Marcia da Fonseca-Martins[6]; Herbert Leonel de Matos Guedes[6,7]; David Mosser[8]; Aloisio Falqueto[9]; Arne Akbar[2] and Daniel Claudio Oliveira Gomes[1,3,4*]

# These authors have contributed equally to this work

[1]Núcleo de Doenças Infecciosas, Universidade Federal do Espírito Santo- Brazil. [2]Instituto de Biofisica Carlos Chagas Filho - Universidade Federal do Rio de Janeiro- Brazil. [3]Division of Medicine, University College London- UK. [4]Núcleo de Biotecnologia, Universidade Federal do Espírito Santo- Brazil. [5]Translational Medicine and Therapeutics, William Harvey Research Institute, Barts and The London School of Medicine and Dentistry, Queen Mary University of London, London, UK; [6]Instituto de Microbiologia Professor Paulo de Goes- Universidade Federal do Rio de Janeiro- Brazil. [7]Instituto Oswaldo Cruz, Fundação Oswaldo Cruz- Brazil. [8]Department of Cell Biology and Molecular Genetics, University of Maryland, College Park, Maryland, USA. [9]Departamento de Medicina Social, Universidade Federal do Espírito Santo- Brazil.

Short Title: Senescent NKG2C+CD57+ cells accumulate in CL

Key Words: Cutaneous leishmaniasis, NK cells, cellular senescence, immunopathology, lesional healing

*Corresponding authors. E-mail address: covrelup@gmail.com and dgomes@ndi.ufes.br

Núcleo de Doenças Infecciosas/ Núcleo de Biotecnologia, Universidade Federal do Espírito Santo – UFES. Av. Marechal Campos, 1468 - Maruípe, Vitória – Brazil. Cep 29043-900.

Tel: +55 27 33357210/ Fax 55 27 33357207

ABSTRACT:

Natural killer (NK) cells include different subsets with diverse effector capacities that are poorly understood in the context of parasitic diseases. Here, we investigated inhibitory and activating receptor expression on NK cells in patients with cutaneous leishmaniasis (CL) and explored their phenotypic and functional heterogeneity based on CD57 and NKG2C expression. The expression of CD57 identified NK cells that accumulated in CL patients and exhibited features of senescence. The $CD57^+$ cells exhibited heightened levels of the activating receptor NKG2C and diminished expression of the inhibitory receptor NKG2A. RNA sequencing analyses based on NKG2C transcriptome have revealed two distinct profiles among CL patients associated with cytotoxic and functional genes. The $CD57^+NKG2C^+$ subset accumulated in the blood of patients and presented conspicuous features of senescence, including the expression of markers such as p16, yH2ax, and p38, as well as reduced proliferative capacity. In addition, they positively correlated with the number of days until lesion resolution. This study provides a broad understanding of the NK cell biology during *Leishmania* infection and reinforces the role of senescent cells in the adverse clinical outcomes of cutaneous leishmaniasis.

INTRODUCTION

Natural killer (NK) cells are innate lymphocytes with a central role in pathogen control and immunosurveillance without a requirement for prior sensitization [1]. They comprise a broad spectrum of subsets with diverse effector capacities, where classically, human NK cells can be classified according to their CD56 expression into a smaller subset of $CD56^{bright}$ and a larger subset of $CD56^{dim}$ NK cells [2] . The $CD56^{dim}$ cytotoxic NK cells differentiate from the $CD56^{bright}$ and have an abundance of cytolytic granules and exhibit spontaneous capacity to lyse tumour and infected target cells [2, 3].

The functional capacity of NK cells depends on their differentiation stage and is modulated by stimuli such as inflammatory mediators and pathogen recognition [4, 5]. End stage differentiation is associated with the acquisition of features of cellular senescence including shortened telomeres, decreased proliferative capacity, and increased expression of the CD57 receptor [6]. This differentiation process also involves changing expression of inhibitory and activating receptors, which leads to phenotypic and functional heterogeneity of NK cells [7, 8]. In this context, the increase in CD57 expression on end-stage NK cells coordinates with a stepwise loss of NKG2A, the parallel increase in KIRs expression and a prominent expression of NKG2C receptor [8–12]. In addition, the simultaneous expression of CD57 and NKG2C is a phenotypic signature of mature NK cells, where the $CD57^{+}NKG2C^{+}$ subset retains the ability to recognize soluble antigens via the NKG2C receptor directly instead of using the canonical NKG2C/HLA-E activation pathway [8, 13]. The $CD57^{+}NKG2C^{+}$ subset have been described as the main responder population to viral infections and can persist for extended periods, suggesting that they may represent the adaptative or “memory-like” NK cell population [14, 15]. However, its role in non-viral infections is very limited.

Recently, we described an enrichment of mature $CD56^{dim}CD57^{+}$ NK cells in patients with cutaneous leishmaniasis that have multiple features of replicative senescence including low proliferative capacity, shorter telomeres, elevated expression of KLRG1 and diminished CD27 co-stimulatory receptor [6]. These cells were expanded in the blood of patients infected with *Leishmania braziliensis* parasites that developed mild localized cutaneous leishmaniasis (CL) [6]. In CL infection, the overwhelming inflammatory and cytotoxicity activity in the infected site are associated with

immunopathology that leads to lesion development [16–18]. Interestingly, compared to senescent cytotoxic CD8⁺ T cells (EMRA), senescent NK cells exhibit pronounced cytotoxicity and inflammatory potential, but lower skin migratory capacity [6]. This suggests that they may play a minor role in lesion pathology. However, given their great inflammatory potential, NK cells have been associated with the maintenance of the systemic inflammatory environment [19–21], which is still unknown in the context of leishmaniasis disease.

Here, we investigate the dynamics of inhibitory and activating receptors expression of the senescent CD57⁺NKG2C⁺ NK cells in the circulation during *L. braziliensis* infection. We found that *L. braziliensis* infection induces a systemic accumulation of senescent CD57⁺NKG2C⁺ NK cells, with a high cytotoxic potential. These cells positively correlated with the number of rounds of treatment until lesion resolution, suggesting that they may participate in the adverse clinical outcome found in CL.

Overall, this study offers comprehensive insights into NK cell biology during *Leishmania* infection and emphasizes the involvement of senescent cells in the unfavourable clinical outcomes of cutaneous leishmaniasis.

MATERIALS & METHODS

Study subjects. Peripheral blood from 16 untreated cutaneous leishmaniasis (CL) patients attending the University Hospital (HUCAM) of Universidade Federal do Espírito Santo, Brazil, were investigated in this study. They consisted of 9 males and 7 females with illness duration ranging from 30 to 120 days and lesion sizes ranging from 200–600 mm^2. The diagnosis of CL was based on clinical and laboratory criteria and all patients in this study were positive for the PCR/restriction fragment length polymorphism of *L. braziliensis* and reported no prior infections or treatment. Upon confirmation of the cutaneous leishmaniasis diagnosis, patients received antimonial chemotherapy treatment following the prescribed protocol established by the Secretaria de Saúde do Estado do Espírito Santo- SESA. Subsequent evaluations were conducted to assess clinical recovery or the necessity for additional treatment rounds, which were administered up to three times until achieving clinical cure. The control group consisted of 16 healthy age and gender-matched individuals (HC) living in a

non-endemic area without a history of leishmaniasis. All study participants (patients and healthy volunteers) were seronegative for HIV, HBV and HCV infections, and had no history of chemotherapy, radiotherapy or treatment with immunosuppressive medications within the last 6 months. They provided written informed consent, and study procedures were performed by the principles of the Declaration of Helsinki. This study was registered at HUCAM ethical committee under referential number 735.274. After sample collection, patients were given standard-of-care treatment (daily intravenous injections of pentavalent antimony; 20 mg/kg per day for 20 days). At day 90 after the start of treatment, patients were evaluated for lesion resolution. The cure was defined as the re-epithelialization of lesions and the resolution of inflamed borders. Patients with active lesions at 90 days were defined as failing treatment and were given an additional round of chemotherapy.

PBMC isolation, cell sorting and culture: PBMC from CL and HC patients were isolated by centrifuging whole blood through a Ficoll-Hypaque (GE Healthcare) gradient followed by hemocytometry to determine the absolute live cell number. NK cells were cultured in complete medium (RPMI-1640 supplemented with 10% heat-inactivated FCS, 100 U/mL penicillin, 100 mg/mL streptomycin, and 2 mM L-glutamine; Invitrogen). NK cells were negatively isolated from PBMC fraction using an NK Cell Isolation Kit/VARIOMACS system (Miltenyi Biotec) according to the manufacturer's instructions.

Flow cytometric analysis. Flow cytometry was performed with the following antibodies: Live/Dead Blue Fixable Stain (L23105, Thermo Scientific), anti-CD3 (UCHT1), anti-CD56 (HCD56) and anti-CD7 (M-T701) were used to identify NK cells. The following antibodies were used to phenotype the NK receptors and differentiation profile: anti-CD16 (3G8), anti-KLRG1 (2F1), anti-CD57 (NK-1), anti-CD158b (CX27), anti-CD158a (HP-3E4), anti-NKG2A (131411), anti-NKG2C (134591), anti-NKG2D (149810), anti-CD161 (191B8), anti-LAIR (DX26). For surface markers, staining was performed at 4°C/30 min in the presence of saturating concentrations of antibodies. For the intracellular analysis

of IFN-γ, granzyme B (GB11), and perforin, cells were fixed and permeabilized with the Fix & Perm® Kit (Invitrogen, Life Technologies, UK). 250 thousand events within live cells gate were acquired for each sample in a Fortessa X-20 cytometer (BD Biosciences) and analysed using FlowJo software (Treestar).

Mitochondrial measurements. Mitochondrial membrane potential was investigated using TMRE (Thermo Fisher), 1 μM TMRE was incubated with PBMCs for 30 min at 37°C, 5% CO_2. Mitochondrial ROS was measured using MitoSOX (Thermo Fisher), 2 μM MitoSOX was incubated with labelled PBMCs for 20 min at 37°C, 5% CO_2. Unfixed samples were immediately collected on a Fortessa X-20 cytometer (BD Biosciences).

Immunofluorescence analysis. Isolated NK cells were deposited on poly-L-lysine coated glass slides by cytocentrifugation (Cytospin, Thermo Scientific, USA). Cytological specimens were then dried and fixed in ethanol/acetone before freezing. Further, specimens were thawed before staining followed by blocking with protein block serum-free reagent (Dako) for 30 minutes. Cells were incubated with primary antibody (Rabbit polyclonal to p-p38 (T180+Y182) Abcam ab38238) overnight at 4°C, followed by 1-hour incubation with conjugated Alexa Fluor® 488-secondary antibody (Invitrogen). Slides were mounted with Vectashield containing DAPI (Vector laboratory). Images were acquired using a Leica SPE2 confocal microscope using LAS X software. Images corresponded to a full Z-stack with 0 5- μm step size and were projected at maximum intensity and analyzed using ImageJ version 2.0.0-rc-43/1.51q.

Western blotting. Lysate of $1x10^6$ isolated NK Cells were washed in PBS and lysed with radio-immunoprecipitation assay (RIPA) buffer (Sigma-Aldrich) supplemented with protease and phosphatase inhibitors (GE Healthcare) for 30 min on ice. Cell lysates (10 or 20 μg of the total protein) were diluted in SDS sample buffer with reducing agent (NuPage, Life Technologies) and boiled for 5

min at 95 °C. Cell lysates were separated by protein electrophoresis at 120 V for 2 h using 10% Bis-Tris pre-cast gels (NuPage) and transferred overnight at 4 °C onto Hybond-P PVDF membranes (GE Healthcare). After blocking, membranes were probed with primary antibodies overnight at 4°C, washed and incubated with HRP-conjugated secondary antibodies (GE Healthcare, 1:4000) for 1 h at room temperature. Antibodies were detected using the ECL detection kit (GE Health-care). Before re-probing with different antibodies, membranes were stripped at 37 °C in agitation using Restore stripping buffer (Thermo Scientific). Primary antibodies were rabbit polyclonal anti-histone γH2A.X (pS139) and anti-p38 MAPK (pThr180/Tyr182) (all from Cell Signaling). All primary antibodies were used at a dilution of 1:1000.

Phosphoflow cytometry. After cell surface staining on ice, cells were fixed with warm Cytofix Buffer (BD Biosciences) for 10 min at 37°C and permeabilized with ice-cold Perm Buffer III (BD Biosciences), followed by staining with the following Abs for 30 min, at room temperature: PE-conjugated antibody to p-16 (BD Pharmingen); Alexa Fluor 488-conjugated antibody to γH2AX phosphorylated at Ser139 (clone 2F3; BioLegemAb (20E3); PE-conjugated antibody to p38 MAPK (Clone 36/p38 (pT180/pY182). Cells were finally washed in Stain Buffer and 250 thousand events within live cells gate were acquired immediately after the stainings on a Fortessa X-20 cytometer (BD Biosciences). Data were analysed using FlowJo v10 software (TreeStar).

Proliferation assay. Sorted NK cells were cultured in the presence rhIL-2 (100 U/mL) for 48h. Ki67 staining was performed (B56; BD Biosciences) with the Foxp3 Staining Set to optimize nuclear staining (Miltenyi Biotec), according to the manufacturer's instructions and analysed by flow cytometry. Supplemented culture medium without rIL-2 was used as control.

RNA sequencing analysis. Raw counts were obtained from a previous study through NCBI's Gene Expression Omnibus repository using accession number: GSE162760 [22]. The study contained data from RNA sequencing of blood of healthy subjects (n = 14) and patients with LC (n = 50). Analyses

were carried out in R v4.2.1 within RStudio [22, 23]. We filtered the dataset for genes with lower than 10 counts in all samples, obtaining a final matrix consisting of 25,957 genes. For differential expression analysis, the DESeq2 package was used [24] and differentially expressed genes were defined as those that had adjusted p-value lower than 0.05. In DESeq2's design formula, we included the batch variable to account for batch effects. For visualization and clustering, the variance stabilizing transformation (vst) was applied to the data through the vst() function in DESeq2 package, and batch effects were removed using removeBatchEffect() function in the limma package. Immune cell deconvolution of bulk data was performed on transformed data as described previously [25] using ImmQuant software with the DMAP reference database. Heatmaps were generated using the ComplexHeatmap package, where clustering was performed with default parameters. The remaining plots related to the RNA-seq analysis were generated using the ggplot2 package (Graphics for Data Analysis. Springer-Verlag New York, 2016).

Statistical comparison of cell scores and gene correlations were also performed in the R environment. Spearman's correlation was calculated between transformed gene expression values and cell population scores predicted by ImmQuant. Relative scores from cell populations inferred by deconvolution were compared using Wilcoxon's rank-sum test, with Benjamini-Hochberg correction. For correlation between gene and cell score data, Spearman's Rank correlation was used. Statistical significance was coded as: *p < 0.05; **p < 0.01; ***p < 0.001; ****p < 0.0001.

Statistics: GraphPad Prism (version 7) was used to perform statistical analysis. Statistical significance was evaluated using the paired Student t-test. Mann-Whitney test was performed for all continuous, nonparametric variables and correlations were calculated using Pearson's correlation coefficient. Spearman's Rank correlation and Receiver Operating Characteristics (ROC) for healing time analyses were performed in the R environment (v. 4.2.2). For the latter, the pROC package (v. 1.18.5) was used. The plots were constructed using the ggplot2 package. Significance was represented as *p <0.05, ** p <0.01, *** p <0.001. Differences were considered significant when p was <0.05.

RESULTS

NK cells from cutaneous leishmaniasis patients exhibit metabolic and molecular features of immunosenescence.

We have previously demonstrated an accumulation of circulating NK cells with multiple features of replicative senescence in CL patients [6]. We extend these observations by demonstrating a significantly increased frequency of phosphorylated p38 protein (p-p38) in NK cells from CL patients compared to controls (Supplementary figure 1A, B). The increased expression of (p-p38) was confirmed by Western blot analysis (Supplementary figure Fig 1C), which also revealed higher expression of DNA damage-related protein yH2Ax (Supplementary figure 1C) in NK cells from CL patients.

Cell bioenergetics play a central role in controlling cellular differentiation processes and the production of inflammatory mediators involved in infections and ageing [26, 27]. In this context, highly differentiated subsets, including senescent cells that acquire inflammatory features, switch their mitochondrial metabolism to a glycolytic state, and this might be used concomitantly with other markers to define changes towards senescence. We therefore accessed the mitochondrial transmembrane potential through TMRE, and we found a hypopolarised phenotype in NK cells from CL patients compared to healthy control subjects (Supplementary figure 1D). In contrast, NK cells of CL patients had higher production of the mitochondrial reactive oxygen species (ROS) (Supplementary Fig 1E). These data support previous observations [6] that indicate NK cells are driven towards senescence by accumulating distinguishable features of molecular and metabolic senescence pathways.

CD57 expression identifies distinct profiles of NK cells in CL patients.

The expression of the CD57 marker has been used to determine senescent or terminally differentiated T and NK cells during ageing or following infections, including leishmaniasis as previously demonstrated by our group [28, 29]. We next investigated the functional and phenotypic profile of CL-NK cells based on the expression of this receptor, which enabled us to discriminate two

distinct subsets $CD56^{dim}CD57^{-}$ and $CD56^{dim}CD57^{+}$ (Supplementary figure 2). We confirmed the accumulation of NK cells expressing $CD57^{+}$ in patients compared to the HC group (Fig. 1A), which displayed a higher cytotoxic potential compared to CD57- subsets (Fig 2B). Both $CD57^{+}$ and CD57- subsets from CL patients had higher production of the mitochondrial reactive oxygen species (ROS) (Fig. 1C). Moreover, the $CD57^{+}$ subset of CL patients demonstrated higher ROS production than the CD57- subset (Fig. 1C). Conversely, both $CD57^{+}$ and $CD57^{-}$ NK cells from CL patients had decreased proportion of hyperpolarized mitochondria compared to the HC group (Fig. 1C). No difference regarding the TMRE analysis was found comparing $CD57^{+}$ and $CD57^{-}$ subsets from both HC and CL groups (Fig. 1C). Together, these data support the idea that $CD57^{+}$ and $CD57^{-}$ NK subsets from CL patients have distinct metabolic requirements.

The differentiation process of NK cells also involves a complex dynamic of inhibitory and activating receptor expression [13, 30, 31], resulting in the observed phenotypic and functional heterogeneity within this population. Previously, we demonstrated the accumulation of $CD57^{+}$ populations during human cutaneous leishmaniasis [6] which was also supported in Figure 1A. Therefore, we next accessed the expression patterns of activating and inhibitory NK receptors within CD57 subsets of CL patients. Our findings indicated that $CD57^{+}$ cells exhibited elevated levels of the activating receptor NKG2C, also observed in complementary analyses of the mean fluorescence intensity (MFI) (Supplementary Figure 3). Similarly, the $CD57^{+}$ subsets demonstrated an increased frequency of KIR2DL2/DL3 (CD158b) expression, while a decreased expression of the inhibitory receptor NKG2A was found in comparison to their CD57-negative counterparts (Fig 1D). Consistent with our previous data [6], the $CD57^{+}$ population demonstrated an increased expression of the differentiation marker KLRG-1 (Fig 1D). No difference was found regarding the frequency expression or MFI of NKG2D, LAIR, CD161 or CD158a (KIR2DL1) (Fig 1D) between CD57 positive and negative subsets. Interestingly, only the NKG2C expression positively correlated with the accumulation of the highly differentiated $NK^{+}CD56dimCD57^{+}$ subset (Fig. 1E), supporting previous findings that suggest that its gain may stand a central stage towards the end differentiated cells.

NKG2C gene expression reveals NK cell profiles with distinct cytotoxic potential in CL patients.

The previous data point to a role for NKR in CL infection [32, 33]. This is further supported by the observation that circulating natural killer cells expressing the activating NKG2C receptor expand during chronic infections and are implicated in the recognition and control of infected cells through cytotoxic function [12, 34, 35]. To evaluate this, we first assessed the NKG2C gene expression profile in the blood of CL patients using RNA-Seq data from a previous study [36]. This revealed two distinct groups, in which one had a low relative expression, and one showed a significantly high expression of NKG2C (Figure 2A).

The gain of NKG2C is associated with increased cytotoxic activity, which is a prominent signature of CL immunopathology [37, 38]. We next evaluated the expression of cytotoxicity genes in the bulk RNA-seq of healthy controls, low NKG2C patients and high NKG2C patients. The expression of cytotoxicity genes (Granzyme A, Granzyme B, Granzyme H and Perforin) showed a significant increase in the high NKG2C group when compared to both the low NKG2C and healthy controls (Figure 2B;C). IFN-γ (*IFNG* gene) demonstrated similar expression between the three groups. In addition, the expression of these cytotoxicity genes was not correlated with the age of patients or the duration of illness (data not shown). Together these suggest the existence of two different profiles of NK cells in patients according to the expression of the NKG2C gene, which are associated with different cytotoxic potentials.

Highly diverse phenotype and function across CD57 and NKG2C NK subsets from CL patients.

As both NKG2C and CD57 expression increased in NK cells in LC patients, and they may be used to identify the NK cell maturation profile within the NK compartment [8, 12, 35], we test whether the acquisition of these markers may be associated with the gain of phenotypic and functional senescence features. As expected, CL patients presented increased frequencies of $CD57^{-}NKG2C^{+}$ and $CD57^{+}NKG2C^{+}$ subsets, while they had lower frequencies of the single $CD57^{+}NKG2C^{-}$ and $CD57^{-}NKG2C^{-}$ subsets when compared to healthy control subjects (Fig 3A and B).

To test whether the acquisition of CD57 and NKG2C may be associated with the gain of phenotypic and functional senescence features, we assessed the expression of key senescence markers and cytotoxic capacity within the four NK cell subsets from CL patients ($CD57^-NKG2C^-$; $CD57^-NKG2C^+$; $CD57^+NKG2C^-$ and $CD57^+NKG2C^+$) (Fig. 3C). The accumulation of p16INK4A/pRB tumour suppressor, an RB family of pocket proteins that act as negative regulators of cell cycle progression were markedly increased in $CD57^+NKG2C^+$ subsets compared with other populations. Furthermore, its expression was higher in the $CD57^+NKG2C^-$ compared to $CD57^-NKG2C^-$ subset (Figure 3C). p38 phosphorylation was increased within $CD57^+NKG2C^+$ cells compared to $CD57^-NKG2C^+$; and $NKG2C^-CD57^-$ subsets (Figure 3C), as well as both $CD57^+NKG2C^+$ and $CD57^+NKG2C^-$ populations demonstrating increased expression of DNA damage-related protein yH2Ax compared to the less differentiated $NKG2C^-CD57^-$ population (Figure 3C). Moreover, we found a gradual increase in proliferative capacity, verified by the cell cycle-related nuclear antigen Ki67 staining within the $CD57^-$subsets ($CD57^-NKG2C^+$ and $NKG2C^-CD57^-$) (Figure 3C). No differences were observed between groups $CD57^+NKG2C^+$ and $CD57^+NKG2C^-$, or even between groups $C57^-NKG2C^+$ and $NKG2C^-CD57^-$.

To complement these phenotypic changes, senescent cells are also characterized by a high functional capacity, represented by gains in secretory and cytotoxic activity. In this scenario, we next investigated granzyme B and perforin production within the NK subsets, which revealed an increased cytotoxic activity associated with the $CD57^+NKG2C^-$ and $CD57^+NKG2C^+$ compared to the less differentiated $CD57^-NKG2C^-$ subset (Fig 3D). However, only $CD57^-NKG2C^+$ cells retained the higher IFN-γ production capacity compared to $CD57^+NKG2C^-$ subset (Fig 3D). Together, these data support that the $CD57^+NKG2C^+$ subset may represent the truly senescent population within the NK compartment. Furthermore, they suggest that the gain of NKG2C is crucial for the acquisition of an NK-educated phenotype with a high proliferative capacity and that these cells move towards senescence with increasing expression of CD57 and acquisition of a highly cytotoxic capacity.

Accumulation of senescent NKG2C$^+$CD57$^+$ subset in patients with lesional healing delay.

NK cell subsets have been employed as indicators of disease severity or treatment success in various infections and tumor treatments [10, 39, 40]. To explore their relevance in the context of LC, we initially correlated the frequency of all subsets with lesional healing time. Interestingly, only the NKG2C$^+$CD57$^+$ subset showed a significant positive correlation with prolonged healing processes, represented by the number of days until lesion resolution in patients (Fig. 4A). Thus, patients with a higher frequency of this cell type exhibited delayed lesional healing, suggesting a potential need for more rounds of treatment compared to those lacking such features of cell differentiation.

To assess prognostic potential, Receiver Operating Characteristic (ROC) curves were plotted for each cell subset, evaluating their ability to distinguish between patient groups. Notably, the NKG2C$^+$CD57$^+$ subset achieved a remarkable combined Area Under the Curve (AUC) of 0.88. Specifically, when discerning between the group with delayed healing (120 days) and the group with a faster healing process (60 days), this subset demonstrated a perfect AUC of 1 (Fig 4B). Crucially, only this subset had all three curves above the ROC AUC threshold (0.5), and the CD57$^+$NKG2C$^-$ subset had the second-highest combined AUC of 0.75 (Supp. Fig. 4). These results corroborate prior findings, emphasizing that the accumulation of senescent cells may impede lesion resolution, thereby negatively impacting CL outcomes.

DISCUSSION

It is well established that infections can promote the expansion of distinct subsets of human NK cells [4, 14, 41]. However, it remains largely unknown how NK cells respond and are regulated during human cutaneous leishmaniasis (CL). A protective function of NK cells is evidenced by the heightened proliferative activity observed in individuals who have been cured compared to those with active lesions [42]. Additionally, elevated frequencies of CD56+ cells are detected in the peripheral blood of CL patients both before and after treatment [43, 44], as well as in the lesions of individuals with Diffuse CL who exhibit a positive response to immunotherapy [45]. Conversely, heightened NK

cell activity is associated with susceptibility and the severity of human visceral leishmaniasis [46], CL [47, 48] and mucocutaneous leishmaniasis [46]. Previously, we have shown that $CD56^{dim}CD57^{+}$ NK subset accumulates in the blood and skin of patients during cutaneous leishmaniasis [6, 25]. These cells presented poor proliferative capacity, high expression of CD57 and KLRG1 and parallel loss of CD27 [49, 50] and therefore, were named as senescent NK population. Here, we extended these data by showing that they also have others senescent features such as increased phosphorylation of p38 map kinase and DNA damage. Moreover, CL-NK cells also demonstrate requirements and stress oxidative potential like those observed in senescent T cells, supporting the idea that these cells may represent a true senescent population within the NK cell compartment.

As human NK cells continuously differentiate, and this process is associated with phenotypical and functional changes driven by inhibitory and activating receptor expression, we access their profile on the CL-$CD56^{dim}CD57^{+}$ expanded cytotoxic cells. We observed an accumulation of NK cells expressing the activating NKG2C and KIR receptors and decreased expression in the NKG2A inhibitory receptor. $CD57^{+}NKG2C^{+}NKG2A^{low}$ NK cells expand and are stably maintained in human blood during ageing or chronic cytomegalovirus (CMV) infection. In our experiments, CL patients and HC volunteers were aged-match and demonstrated the exact prevalence of CMV-positive serology. This suggests that the senescent $CD57^{+}NKG2C^{+}NKG2A^{low}$ subset that expanded during CL infection was driven by other factors, which require further investigation.

Cytotoxicity-related gene expression is one of the main signatures found in the skin and blood of CL patients [36–38, 51]. We found that NKG2C gene expression may differentiate two distinct populations, whereby high levels of NKG2C expression correlated with an abundance of cytolytic markers. This relationship was also observed in relation to CD57 expression [6]. In fact, the mature NK cell compartments can be stratified by using both CD57 and/or NKG2C expression[8, 12, 35, 52, 53]. Therefore, $NKG2C^{+}$ NK cells were expanded in CL patients and represented a subset with increased IFN-γ and active proliferation, while $CD57^{+}NKG2C^{+}$ subsets retained classical senescent markers such as p16, p38 and yH2Ax alongside a low proliferative capacity. Moreover, the gain of

both CD57 and NKG2C was linked with remarkable frequency of cytotoxic granules, suggesting that these receptors may be related to each other during the differentiation process, which was corroborated by the positive correlation between CD57 and NKG2C, as demonstrated here.

$CD57^+NKG2C^+$ expand during viral infections and are critical in controlling viremia through intense inflammatory and cytotoxic activity [11, 12, 54, 55] . In this regard, our data raises a question about the importance of this senescent NK subset expansion in the blood of patients during *Leishmania* infection seeing that parasites are mainly restricted to skin and draining lymph nodes. We have previously demonstrated that although circulating CL-NK cells exhibited a high cytotoxic and inflammatory potential, they presented lower skin-homing capacity than senescent T cells [6]. Thus, it is possible that while senescent T cells play a pathogenic role in the skin, senescent $CD57^+NKG2C^+$ NK cells that accumulate in the blood maintain the systemic inflammatory environment as observed in CL patients. In line with this, the adoptive transfer of mature-NK cells is efficient against haematological malignancies, but less promising in targeting solid tumours due to their poor migratory and infiltration capacities [56]. Interestingly, as $NKG2C^+CD57^+$ NK cells retain the potential to be maintained and stimulated through exposure to homeostatic and inflammatory cytokines [57, 58], the systemic inflammatory environment may also act in the positive feedback looping towards the differentiation of these senescent NK populations.

CL patients that develop chronic ulcerated lesions often fail to respond to the pentavalent antimony drug treatment, resulting in the need for additional rounds of treatment until clinical cure [59]. Thus, many factors may affect the cure rate, including immunological factors such as high expression of cytolytic genes (GZMB, PRF1 and GNLY) [60]. Our data points to an increase in the $NKG2C^+CD57^+$ population, which accumulated in patients with lesional healing delay. NK cell subsets have been employed as indicators of disease severity or treatment success in various infections and tumor treatment [10, 39, 40]. In this scenario, the circulating estimation of senescent NKG2C+CD57+ subset frequency may have potential use in estimating CL's severity, which still requires further investigation.

Collectively, our findings expand the comprehension of NK cell biology during cutaneous leishmaniasis and identify a senescent NKG2C+CD57+ NK subset that accumulates in patients with therapeutic failure. The growing body of evidence implicating senescent cells in CL pathogenesis underscores the imperative to explore the role of senescent cells as a potential target for therapy against leishmaniasis and other related pathologies.

ETHICAL APPROVAL: This study involving human participants was reviewed and approved by the ethics committee of Hospital Universitário Cassiano de Moraes- HUCAM/ Universidade Federal do Espírito Santo. All participants provided their written in- informed consent to participate in this study.

ACKNOWLEDGMENTS: Authors would like to thank Dr. Olivia Bracken (Medicine Division, University College London- UK) for the scientific discussion and paper formatting.

FUNDING: DCOG is supported by Fundação de Amparo a Pesquisa do Espírito Santo- FAPES (Grant 1006/2022) and National Council for Scientific and Technological Development-CNPQ (Grant 200222/2022-8). ANA is supported by grants MR/T015853/1, MR/T030534/1 and MR/P00184X/1 from the Medical Research Council (UK). LPC is supported by Coordenação de Aperfeiçoamento de Pessoal de Nível Superior - Brasil (CAPES) - Finance Code 001 and *Fundação Carlos Chagas Filho de Amparo à Pesquisa do Estado do Rio de Janeiro* (FAPERJ-PDS-2023).

CONFLICT OF INTEREST: The authors state no conflict of interest.

AUTHOR CONTRIBUTIONS: LC., AA and DG. conceived and designed the work. LC., CF., PM. and AF. performed the experiments. AF., PM., AQ., JF. and HG. enrolled patients and collected clinical data. LC and CF performed the statistical analysis. DM., SH., AA., LC and DG. wrote the manuscript. All authors contributed to the article, critically revised the manuscript and approved the submitted version. All contributors to this study are listed as co-authors.

DATA AVAILABILITY: The raw data supporting the conclusions of this article will be made available by the authors, without undue reservation.

REFERENCES:

1. Jaeger BN, Vivier E. When NK cells overcome their lack of education. Journal of Clinical Investigation. 2012;122:3053–6.

2. Melsen JE, Lugthart G, Lankester AC, Schilham MW. Human Circulating and Tissue-Resident CD56bright Natural Killer Cell Populations. Front Immunol. 2016;7 JUN.

3. Ouyang Q, Baerlocher G, Vulto I, Lansdorp PM. Telomere length in human natural killer cell subsets. In: Annals of the New York Academy of Sciences. 2007.

4. Luetke-Eversloh M, Killig M, Romagnani C. Signatures of human NK cell development and terminal differentiation. Front Immunol. 2013;4 DEC:1–6.

5. Bengsch B, Ohtani T, Herati RS, Bovenschen N, Chang KM, Wherry EJ. Deep immune profiling by mass cytometry links human T and NK cell differentiation and cytotoxic molecule expression patterns. J Immunol Methods. 2018;453:3–10.

6. Covre LP, Devine OP, Garcia de Moura R, Vukmanovic-Stejic M, Dietze R, Ribeiro-Rodrigues R, et al. Compartmentalized cytotoxic immune response leads to distinct pathogenic roles of natural killer and senescent CD8+ T cells in human cutaneous leishmaniasis. Immunology. 2020;159:429–40.

7. Lanier LL. Natural killer cell receptor signaling. Current Opinion in Immunology. 2003;15.

8. Björkström NK, Riese P, Heuts F, Andersson S, Fauriat C, Ivarsson M a, et al. Expression patterns of NKG2A, KIR, and CD57 define a process of CD56dim NK cell differentiation uncoupled from NK cell education. Blood. 2010;116:3853–64.

9. Highton AJ, Diercks BP, Möckl F, Martrus G, Sauter J, Schmidt AH, et al. High Metabolic Function and Resilience of NKG2A-Educated NK Cells. Front Immunol. 2020;11.

10. Ma M, Wang Z, Chen X, Tao A, He L, Fu S, et al. NKG2C+NKG2A- natural killer cells are associated with a lower viral set point and may predict disease progression in individuals with primary HIV infection. Front Immunol. 2017;8 SEP.

11. Kared H, Martelli S, Tan SW, Simoni Y, Chong ML, Yap SH, et al. Adaptive NKG2C+CD57+ natural killer cell and Tim-3 expression during viral infections. Front Immunol. 2018;9 APR.

12. Heath J, Newhook N, Comeau E, Gallant M, Fudge N, Grant M. NKG2C $^{+}$ CD57 $^{+}$ Natural Killer Cell Expansion Parallels Cytomegalovirus-Specific CD8 $^{+}$ T Cell Evolution towards Senescence. J Immunol Res. 2016;2016:1–8.

13. Lopez-Vergès S, Milush JM, Pandey S, York VA, Arakawa-Hoyt J, Pircher H, et al. CD57 defines a functionally distinct population of mature NK cells in the human CD56dimCD16+ NK-cell subset. Blood. 2010;116:3865–74.

14. Sheppard S, Sun JC. Virus-specific NK cell memory. Journal of Experimental Medicine. 2021;218.

15. Pahl JHW, Cerwenka A, Ni J. Memory-Like NK cells: Remembering a previous activation by cytokines and NK cell receptors. Frontiers in Immunology. 2018;9 NOV.

16. Faria DR, Souza PEA, Durães F V., Carvalho EM, Gollob KJ, MacHado PR, et al. Recruitment of CD8+ T cells expressing granzyme A is associated with lesion progression in human cutaneous leishmaniasis. Parasite Immunol. 2009;31:432–9.

17. Scott P, Novais FO. Cutaneous leishmaniasis: Immune responses in protection and pathogenesis. Nature Reviews Immunology. 2016;16:581–92.

18. Novais FO, Carvalho LP, Graff JW, Beiting DP, Ruthel G, Roos DS, et al. Cytotoxic T Cells Mediate Pathology and Metastasis in Cutaneous Leishmaniasis. PLoS Pathog. 2013;9.

19. Picard E, Armstrong S, Andrew MK, Haynes L, Loeb M, Pawelec G, et al. Markers of systemic inflammation are positively associated with influenza vaccine antibody responses with a possible role for ILT2(+)CD57(+) NK-cells. Immunity and Ageing. 2022;19.

20. Kleinertz H, Hepner-Schefczyk M, Ehnert S, Claus M, Halbgebauer R, Boller L, et al. Circulating growth/differentiation factor 15 is associated with human CD56bright natural killer cell dysfunction and nosocomial infection in severe systemic inflammation. EBioMedicine. 2019;43.

21. Bluman EM, Bartynski KJ, Avalos BR, Caligiuri MA. Human natural killer cells produce abundant macrophage inflammatory protein-1α in response to monocyte-derived cytokines. Journal of Clinical Investigation. 1996;97.

22. RStudio Team. RStudio: Integrated Development for R. RStudio, Inc., Boston, MA. 2021.

23. R Core Team. R Core Team 2021 R: A language and environment for statistical computing. R foundation for statistical computing. https://www.R-project.org/. R Foundation for Statistical Computing. 2022;2.

24. Love MI, Huber W, Anders S. Moderated estimation of fold change and dispersion for RNA-seq data with DESeq2. Genome Biol. 2014;15:1–21.

25. Fantecelle CH, Covre LP, Garcia de Moura R, Guedes HL de M, Amorim CF, Scott P, et al. Transcriptomic landscape of skin lesions in cutaneous leishmaniasis reveals a strong CD8+ T cell immunosenescence signature linked to immunopathology. Immunology. 2021;164.

26. Henson SM, Lanna A, Riddell NE, Franzese O, Macaulay R, Griffiths SJ, et al. p38 signaling inhibits mTORC1-independent autophagy in senescent human CD8+ T cells. J Clin Invest. 2014;124:1–13.

27. Mittelbrunn M, Kroemer G. Hallmarks of T cell aging. Nature Immunology. 2021;22.

28. Covre LP, Martins RF, Devine OP, Chambers ES, Vukmanovic-Stejic M, Silva JA, et al. Circulating senescent T cells are linked to systemic inflammation and lesion size during human cutaneous leishmaniasis. Front Immunol. 2019;10 JAN:1–12.

29. Moura RG De, Covre LP, Fantecelle CH, Alejandro V, Gajardo T, Cunha CB, et al. PD-1 Blockade Modulates Functional Activities of Exhausted-Like T Cell in Patients With Cutaneous Leishmaniasis. 2021;12 March:1–12.

30. Nikzad R, Angelo LS, Aviles-Padilla K, Le DT, Singh VK, Bimler L, et al. Human natural killer cells mediate adaptive immunity to viral antigens. 2019.

31. Poznanski SM, Ashkar AA. What defines NK cell functional fate: Phenotype or metabolism? Frontiers in Immunology. 2019;10 JUN.

32. Crosby EJ, Goldschmidt MH, Wherry EJ, Scott P. Engagement of NKG2D on Bystander Memory CD8 T Cells Promotes Increased Immunopathology following Leishmania major Infection. PLoS Pathog. 2014;10:e1003970.

33. Sacramento LA, Farias Amorim C, Campos TM, Saldanha M, Arruda S, Carvalho LP, et al. NKG2D promotes CD8 T cell-mediated cytotoxicity and is associated with treatment failure in human cutaneous leishmaniasis. PLoS Negl Trop Dis. 2023;17:e0011552.

34. Marquardt N, Ivarsson MA, Blom K, Gonzalez VD, Braun M, Falconer K, et al. The Human NK Cell Response to Yellow Fever Virus 17D Is Primarily Governed by NK Cell Differentiation Independently of NK Cell Education. The Journal of Immunology. 2015;195:3262–72.

35. Kared H, Martelli S, Tan SW, Simoni Y, Chong ML, Yap SH, et al. Adaptive NKG2C+CD57+ Natural Killer Cell and Tim-3 Expression During Viral Infections. Front Immunol. 2018;9.

36. Farias Amorim C, Novais FO, Nguyen BT, Nascimento MT, Lago J, Lago AS, et al. Localized skin inflammation during cutaneous leishmaniasis drives a chronic, systemic ifn-γ signature. PLoS Negl Trop Dis. 2021;15.

37. Novais FO, Carvalho LP, Passos S, Roos DS, Carvalho EM, Scott P, et al. Genomic Profiling of Human Leishmania braziliensis Lesions Identifies Transcriptional Modules Associated with Cutaneous Immunopathology. Journal of Investigative Dermatology. 2015;135:94–101.

38. Christensen SM, Dillon LAL, Carvalho LP, Passos S, Novais FO, Hughitt VK, et al. Meta-transcriptome Profiling of the Human-Leishmania braziliensis Cutaneous Lesion. PLoS Negl Trop Dis. 2016;10:1–17.

39. Sun C, Xu J, Huang Q, Huang M, Wen H, Zhang C, et al. High NKG2A expression contributes to NK cell exhaustion and predicts a poor prognosis of patients with liver cancer. Oncoimmunology. 2017;6.

40. Pascual-Guardia S, Ataya M, Ramírez-Martínez I, Yélamos J, Chalela R, Bellido S, et al. Adaptive NKG2C+ natural killer cells are related to exacerbations and nutritional abnormalities in COPD patients. Respir Res. 2020;21.

41. Tschan-Plessl A, Stern M, Schmied L, Retière C, Hirsch HH, Garzoni C, et al. Human Cytomegalovirus Infection Enhances NK Cell Activity in Vitro. Transplant Direct. 2016;2:E89.

42. Maasho K, Sanchez F, Schurr E, Hailu A, Akuffo H. Indications of the protective role of natural killer cells in human cutaneous leishmaniasis in an area of endemicity. Infect Immun. 1998;66:2698–704.

43. Cunha CF, Ferraz R, Pimentel MIF, Lyra MR, Schubach AO, Da-Cruz AM, et al. Cytotoxic cell involvement in human cutaneous leishmaniasis: Assessments in active disease, under therapy and after clinical cure. Parasite Immunol. 2016;38:244–54.

44. Cunha CF, Ferraz-Nogueira R, Costa VFA, Pimentel MIF, Chometon TQ, Lyra MR, et al. Contribution of Leishmania braziliensis antigen-specific CD4+ T, CD8+ T, NK and CD3+CD56+NKT cells in the immunopathogenesis of cutaneous leishmaniasis patients: Cytotoxic, activation and exhaustion profiles. PLoS One. 2020;15.

45. Pereira LIA, Dorta ML, Pereira AJCS, Bastos RP, Oliveira MAP, Pinto SA, et al. Case report: Increase of NK cells and proinflammatory monocytes are associated with the clinical improvement of diffuse cutaneous leishmaniasis after immunochemotherapy with BCG/Leishmania antigens. American Journal of Tropical Medicine and Hygiene. 2009;81:378–83.

46. Manna PP, Bharadwaj D, Bhattacharya,' S, Chakrabarti G, Basu D, Kumar Mallik K, et al. Impairment of Natural Killer Cell Activity in Indian Kala-Azar: Restoration of Activity by Interleukin 2 but Not by Alpha or Gamma Interferon. 1993.

47. Ferraz R, Cunha CF, Pimentel MIF, Lyra MR, Pereira-Da-Silva T, Schubach AO, et al. CD3+CD4negCD8neg (double negative) T lymphocytes and NKT cells as the main cytotoxic-related-CD107a+ cells in lesions of cutaneous leishmaniasis caused by Leishmania (Viannia) braziliensis. Parasit Vectors. 2017;10:219.

48. Campos TM, Novais FO, Saldanha M, Costa R, Lordelo M, Celestino D, et al. Granzyme B Produced by Natural Killer Cells Enhances Inflammatory Response and Contributes to the Immunopathology of Cutaneous Leishmaniasis. Journal of Infectious Diseases. 2020;221:973–82.

49. Müller-Durovic B, Lanna A, Polaco Covre L, Mills RS, Henson SM, Akbar AN. Killer Cell Lectin-like Receptor G1 Inhibits NK Cell Function through Activation of Adenosine 5′-Monophosphate–Activated Protein Kinase. The Journal of Immunology. 2016;197:2891–9.

50. Morgado S, Sanchez-Correa B, Casado JG, Duran E, Gayoso I, Labella F, et al. NK cell recognition and killing of melanoma cells is controlled by multiple activating receptor-ligand interactions. J Innate Immun. 2011;3:365–73.

51. Amorim CF, Novais FO, Nguyen BT, Misic AM, Carvalho LP, Carvalho EM, et al. Variable gene expression and parasite load predict treatment outcome in cutaneous leishmaniasis. Sci Transl Med. 2019;11.

52. Lopez-Vergès S, Milush JM, Schwartz BS, Pando MJ, Jarjoura J, York V a, et al. Expansion of a unique CD57+NKG2Chi natural killer cell subset during acute human cytomegalovirus infection. Proc Natl Acad Sci U S A. 2011;108:14725–32.

53. Kobyzeva PA, Streltsova MA, Erokhina SA, Kanevskiy LM, Telford WG, Sapozhnikov AM, et al. CD56dimCD57−NKG2C+ NK cells retaining proliferative potential are possible precursors of CD57+NKG2C+ memory-like NK cells. J Leukoc Biol. 2020;108:1379–95.

54. Hendricks DW, Balfour HH, Dunmire SK, Schmeling DO, Hogquist KA, Lanier LL. Cutting Edge: NKG2ChiCD57+ NK Cells Respond Specifically to Acute Infection with Cytomegalovirus and Not Epstein–Barr Virus. The Journal of Immunology. 2014;192:4492–6.

55. Foley B, Cooley S, Verneris MR, Curtsinger J, Luo X, Waller EK, et al. Human Cytomegalovirus (CMV)-Induced Memory-like NKG2C+ NK Cells Are Transplantable and Expand In Vivo in Response to Recipient CMV Antigen. The Journal of Immunology. 2012;189:5082–8.

56. Velichinskii RA, Streltsova MA, Kust SA, Sapozhnikov AM, Kovalenko EI. The biological role and therapeutic potential of nk cells in hematological and solid tumors. International Journal of Molecular Sciences. 2021;22.

57. Sun JC, Lanier LL. NK cell development, homeostasis and function: Parallels with CD8 + T cells. Nature Reviews Immunology. 2011;11.

58. Tarannum M, Romee R. Cytokine-induced memory-like natural killer cells for cancer immunotherapy. Stem Cell Research and Therapy. 2021;12.

59. Olías-molero AI, de la Fuente C, Cuquerella M, Torrado JJ, Alunda JM. Antileishmanial drug discovery and development: Time to reset the model? Microorganisms. 2021;9.

60. Amorim CF, Novais FO, Nguyen BT, Misic AM, Carvalho LP, Carvalho EM, et al. Variable gene expression and parasite load predict treatment outcome in cutaneous leishmaniasis. 2019.

Legend to figures

Figure 1. CD57 expression identifies distinct phenotypic and metabolic profiles of NK cells in CL patients. (A) Expression of CD57 marker in total $CD56^{dim}$NK cells from aged-matched healthy controls (HC=14) and cutaneous leishmaniasis patients (CL=14). (B) Ex vivo granzyme B production (C) Cumulative data of MitoSOX and TMRE stainings. (D) Expression of NK receptors within $CD56^{dim}$NK cells from CL patients, stratified by CD57 expression. (E) Scatterplot showing Spearman's correlation test relationship between frequencies of $NK^{+}CD56^{dim}CD57^{+}$ cells and NK receptors expression from CL patients. The graphs show median with 95% of confidence. The p values were calculated using Mann Whitney or Kruskal-Wallis test with Dunn´s correction for multiple comparisons. *p <0.05, ** p <0.01, *** p <0.001.

Figure 2. Blood gene expression reveals two profiles of NKG2C expression associated with distinct cytotoxicity levels. (A) Relative NKG2C gene expression. Expression of selected genes (GZMA, GZMB, GZMH, IFNG, KLRC2, PRF1) through (B) a heatmap and (C) violin plots, where some patients show NKG2C gene expression compared to those of controls (Low NKG2C patients) and display lower levels of cytotoxicity. HC: Healthy controls. *: $p < 0.05$; **: $p < 0.01$; ***: $p < 0.001$; ****: $p < 0.0001$. Gene expression values are on the log2 scale and heatmap shows relative expression values centred around the mean.

Figure 3. Phenotype and function across CD57 and NKG2C NK subsets from CL patients. (A) Representative plots and (B) cumulative data of percentage of NK subsets stratified by CD57 and NKG2C expression. Violin plots of cumulative data of MFI of (C) p16, γH2AX and p-p38 MAPK expressions and fold change of Ki67 frequency within NK cell subsets from CL patients. (D) Violin plots of the cumulative data of the percentage of granzyme B, perforin and IFN-γ within NK subsets from CL patients. The graphs show median with 95% confidence. The p-values were calculated using Mann Whitney test or Friedman test with Dunn´s correction for multiple comparisons. *p <0.05, ** p <0.01, *** p <0.001

Figure 4. Increased frequency of the NKG2C$^+$CD57$^+$ are associated with lesional delayed healing. A) Spearman's rank correlation (ρ) between cell frequencies and patient healing time, and B) Receiver Operating Characteristics curves for the NKG2C$^+$CD57$^+$ subset for each group comparison and the combined (multiclass) Area Under Curve (AUC). "x<y" represents the ability of distinguishing between the Y healing time (days) and the X healing time (days), according to the groups defined in the legend. *p <0.05, ** p <0.01, *** p <0.001.

Supplementary figure 1. Circulating NK cells from CL patients exhibit metabolic and molecular features of immunosenescence. Purified NK cells (over 95% of purity) from HC (n=5) and CL (n=5) groups were isolated from PBMC without stimulation. (A) Immunofluorescence staining for the expression of p38MAPK (pThr180/Tyr182) (green). Nuclei were counterstained with DAPI (blue). Scale bars, 100 μM. (B). Cumulative data of p38MAPK expression analysed by immunofluorescence. (C) Representative western blot performed on lysates from NK cells showing the phosphorylation of p38MAPK (pThr180/Tyr182) and yH2AX (pser139) GAPDH served as loading control. Numbers indicate molecular weights (kDa) of blotted proteins. (D) Representative flow cytometry histograms and cumulative data of TMRE staining. (F) Representative flow cytometry histograms and cumulative data of

MitoSOX staining. The graphs show median with 95% of confidence. The p values were calculated using Mann Whitney test. *p <0.05, ** p <0.01, *** p <0.001.

Supplementary figure 2. **Representative gate strategy.** (A) NK cells were identified from PBMC by gating on lymphocytes, single cells, live cells, CD3-negative and CD7-positive cells, representing the total NK cells. The $CD56^{dim}$NK cells were then stratified into 2 subsets accordingly to CD57 expression, representing $CD57^-$ and $CD57^+$ cells.

Supplementary Figure 3. Expression of NK receptors within $CD56^{dim}$NK cells from CL patients, stratified by CD57 expression. Cumulative data of mean fluorescence intensity (MFI) of NKG2C, NKG2D, CD158a, CD158b, KLRG1, LAIR, NKG2A, CD161. The graphs show median with 95% of confidence. The p values were calculated using Mann Whitney test. *p <0.05, ** p <0.01, *** p <0.001.

Supplementary Figure 4. Less differentiated NK cell subsets do not display a conspicuous ability to distinguish healing time of CL patients. Here are shown Receiver Operating Characteristics curves for the $CD57^-NKG2C^+$, $CD57^+NKG2C^-$ and $NKG2C^-CD57^-$ subsets for each group comparison and the respective combined (multiclass) Area Under Curve (AUC). "x<y" represents the ability of distinguishing between the Y days group and the X days group, according to the groups in the legend.

Abstract graphic. (A) NK subsets present opposite immune and senescence features in cutaneous leishmaniasis. (B) Expansion of cytotoxic NKG2C+CD57+ NK cells is associated with increased lesional healing dalay. Spearman's rank correlation (ρ) between cell subsets frequencies and patient stratified by CD57 and NKG2C expression and lesional healing time (days) taken by cutaneous leishmaniasis patients. The graphs show median with 95% confidence. The p values were calculated by comparing each treatment round set between the NK cell subsets using RM-one way ANOVA and Benjamin and Hochberg method. *p <0.05, ** p <0.01, *** p <0.001.

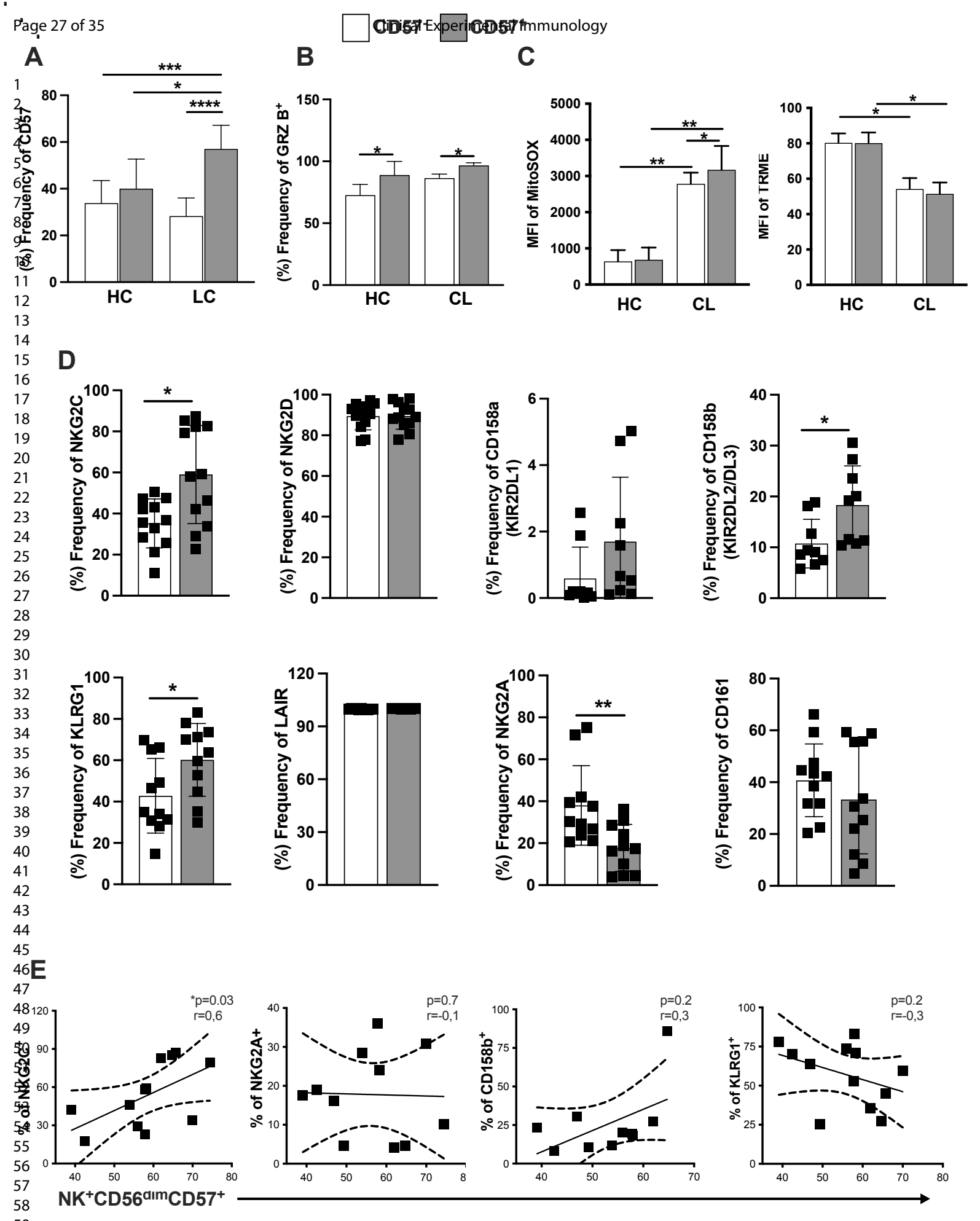
CD57⁻
CD57⁺
A
(%) Frequency of CD57
HC
LC
B
(%) Frequency of GRZ B⁺
HC
CL
C
MFI of MitoSOX
HC
CL
MFI of TRME
HC
CL
D
(%) Frequency of NKG2C
(%) Frequency of NKG2D
(%) Frequency of CD158a (KIR2DL1)
(%) Frequency of CD158b (KIR2DL2/DL3)
(%) Frequency of KLRG1
(%) Frequency of LAIR
(%) Frequency of NKG2A
(%) Frequency of CD161
E
*p=0.03
r=0,6
p=0.7
r=-0,1
p=0.2
r=0,3
p=0.2
r=-0,3
% of NKG2C+
% of NKG2A+
% of CD158b+
% of KLRG1+
NK+CD56dimCD57+

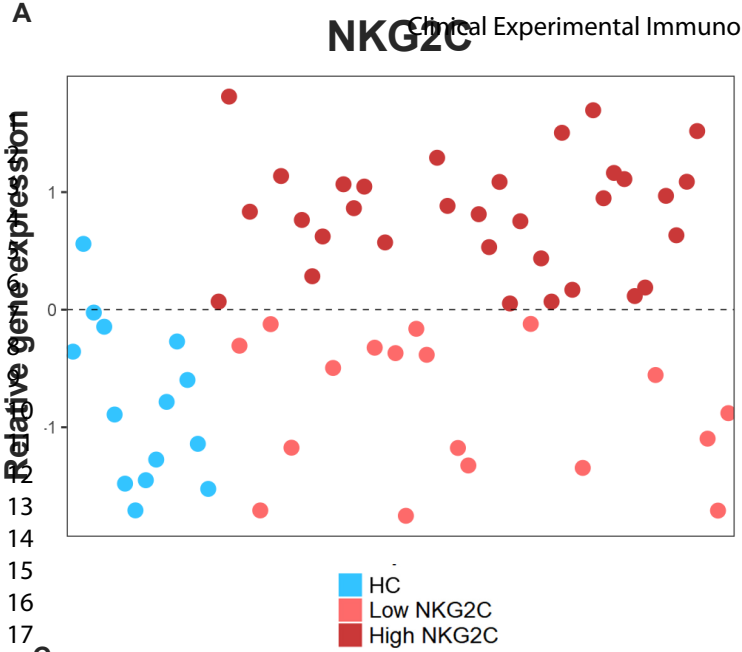
A
NKG2C
Relative gene expression
1
0
-1
HC
Low NKG2C
High NKG2C

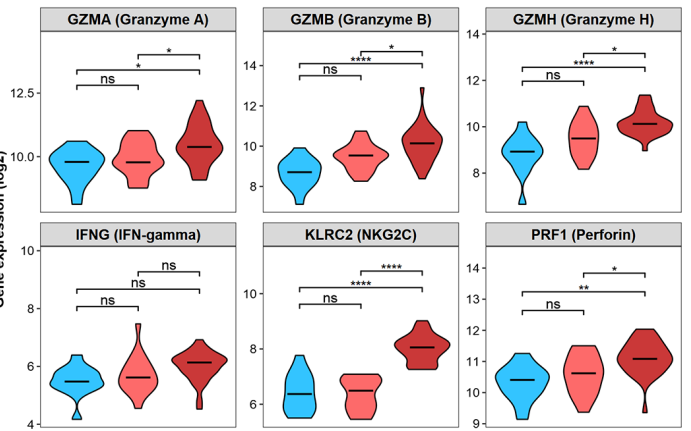
C
GZMA (Granzyme A)
GZMB (Granzyme B)
GZMH (Granzyme H)
IFNG (IFN-gamma)
KLRC2 (NKG2C)
PRF1 (Perforin)
Gene expression (log2)
ns
*
**
****

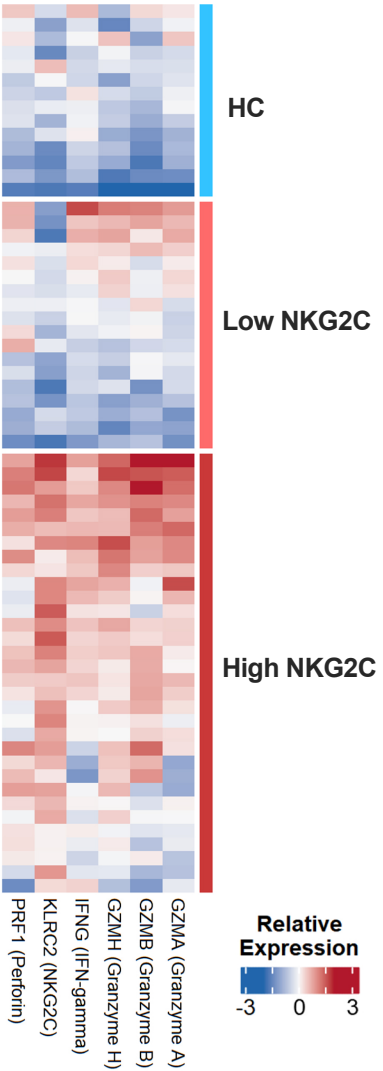
B
HC
Low NKG2C
High NKG2C
PRF1 (Perforin)
KLRC2 (NKG2C)
IFNG (IFN-gamma)
GZMH (Granzyme H)
GZMB (Granzyme B)
GZMA (Granzyme A)
Relative Expression
-3
0
3

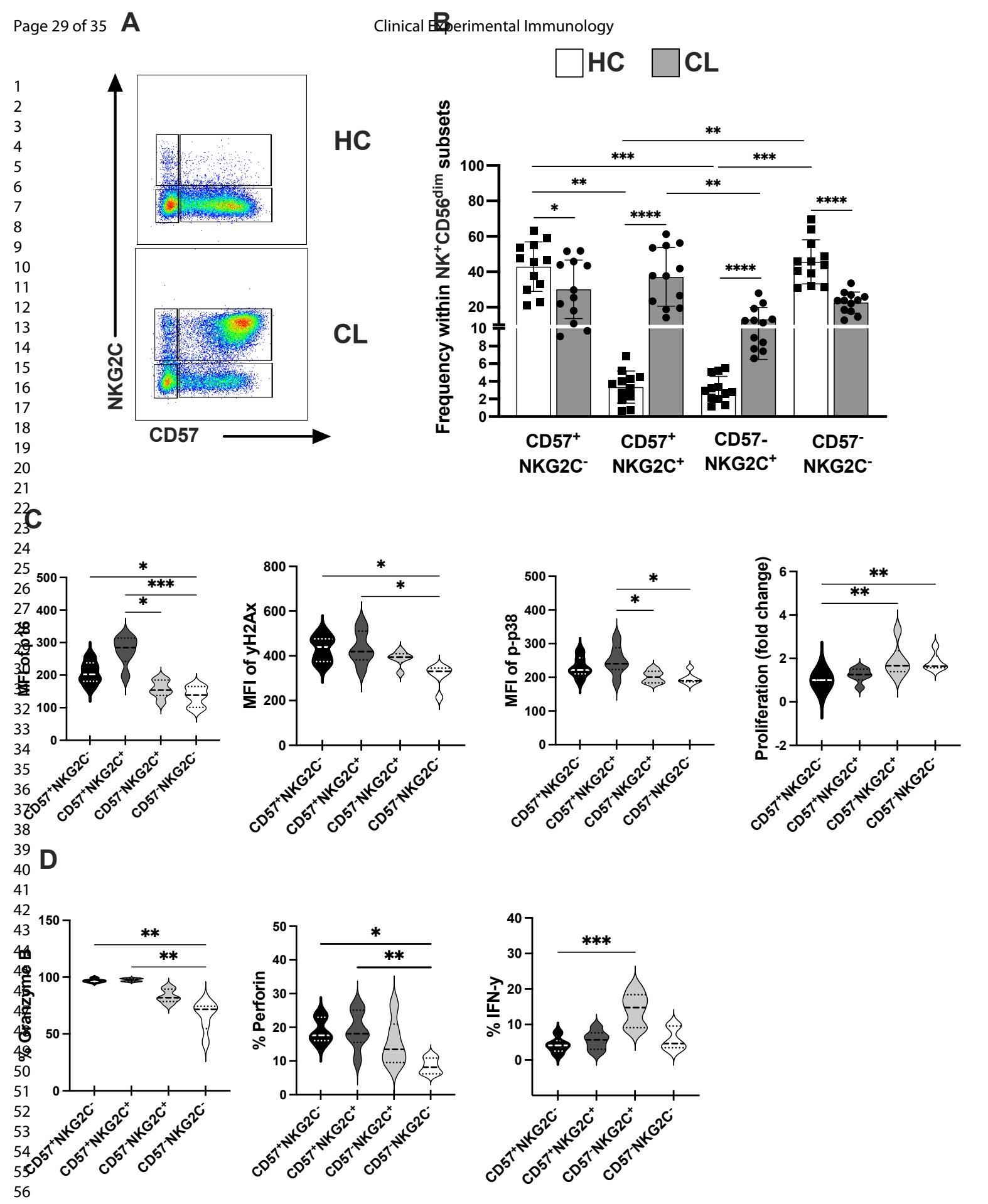
A
HC
CL
NKG2C
CD57
B
HC
CL
Frequency within NK+CD56dim subsets
CD57+ NKG2C-
CD57+ NKG2C+
CD57- NKG2C+
CD57- NKG2C-
C
MFI of p-p38
MFI of yH2Ax
MFI of p-p38
Proliferation (fold change)
CD57+NKG2C-
CD57+NKG2C+
CD57-NKG2C+
CD57-NKG2C-
D
% Granzyme B
% Perforin
% IFN-γ

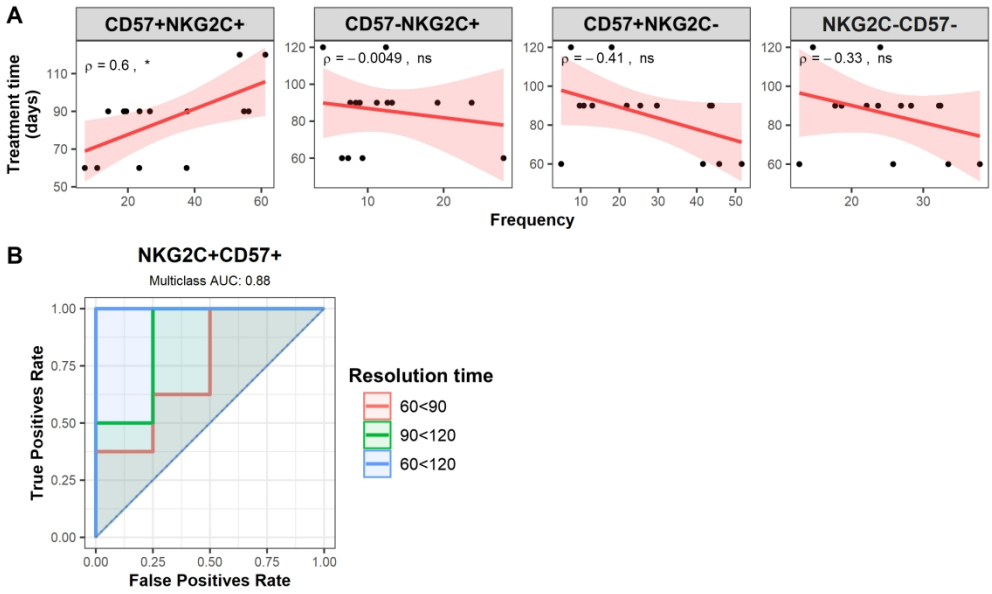

881x529mm (72 x 72 DPI)

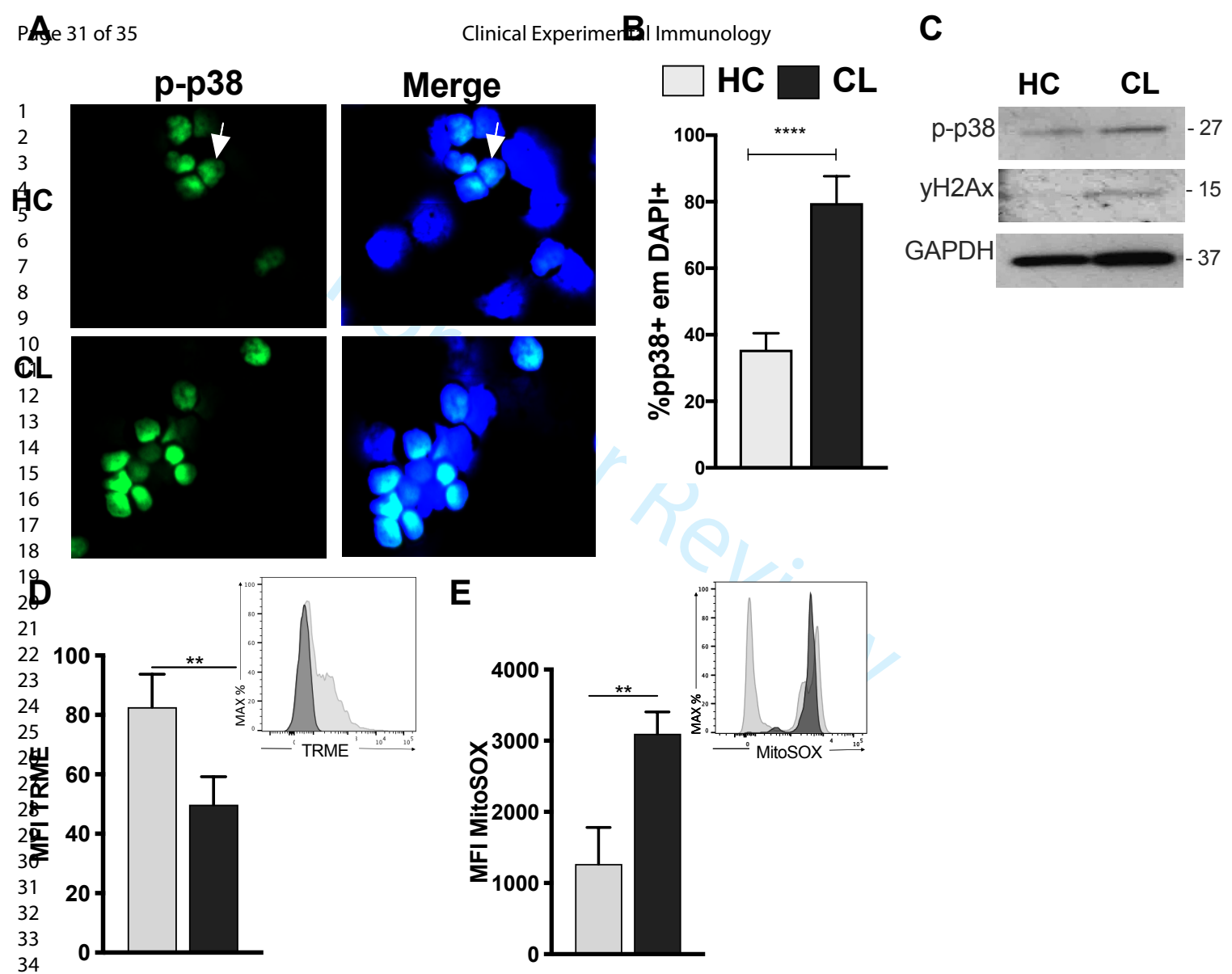
A
p-p38
Merge
HC
CL
B
HC
CL
%pp38+ em DAPI+
****
C
HC
CL
p-p38
yH2Ax
GAPDH
- 27
- 15
- 37
D
MFI TRME
**
MAX %
TRME
E
MFI MitoSOX
**
MAX %
MitoSOX

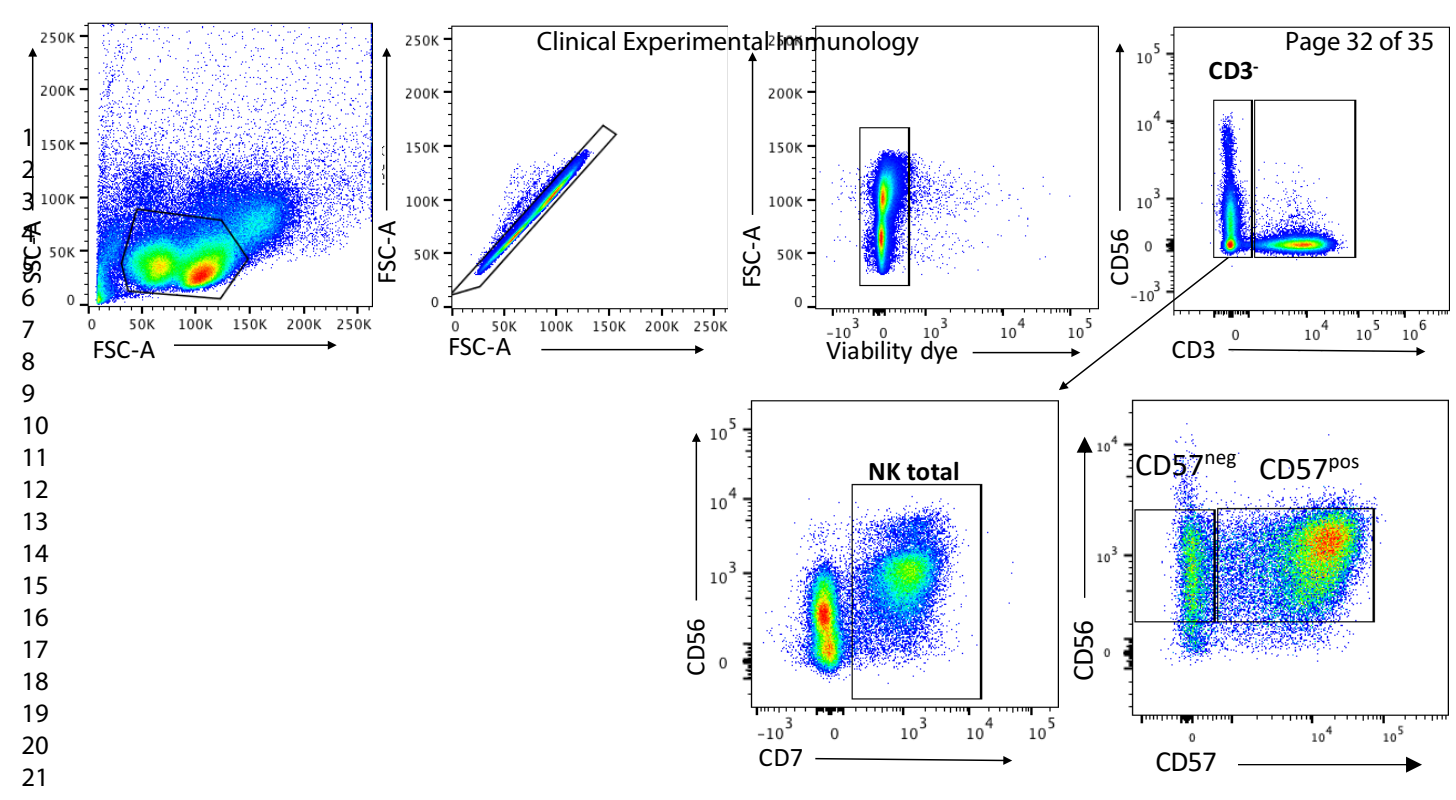
SSC-A
FSC-A
FSC-A
FSC-A
FSC-A
Viability dye
CD56
CD3
CD3-
NK total
CD7
CD56
CD57neg
CD57pos
CD56
CD57

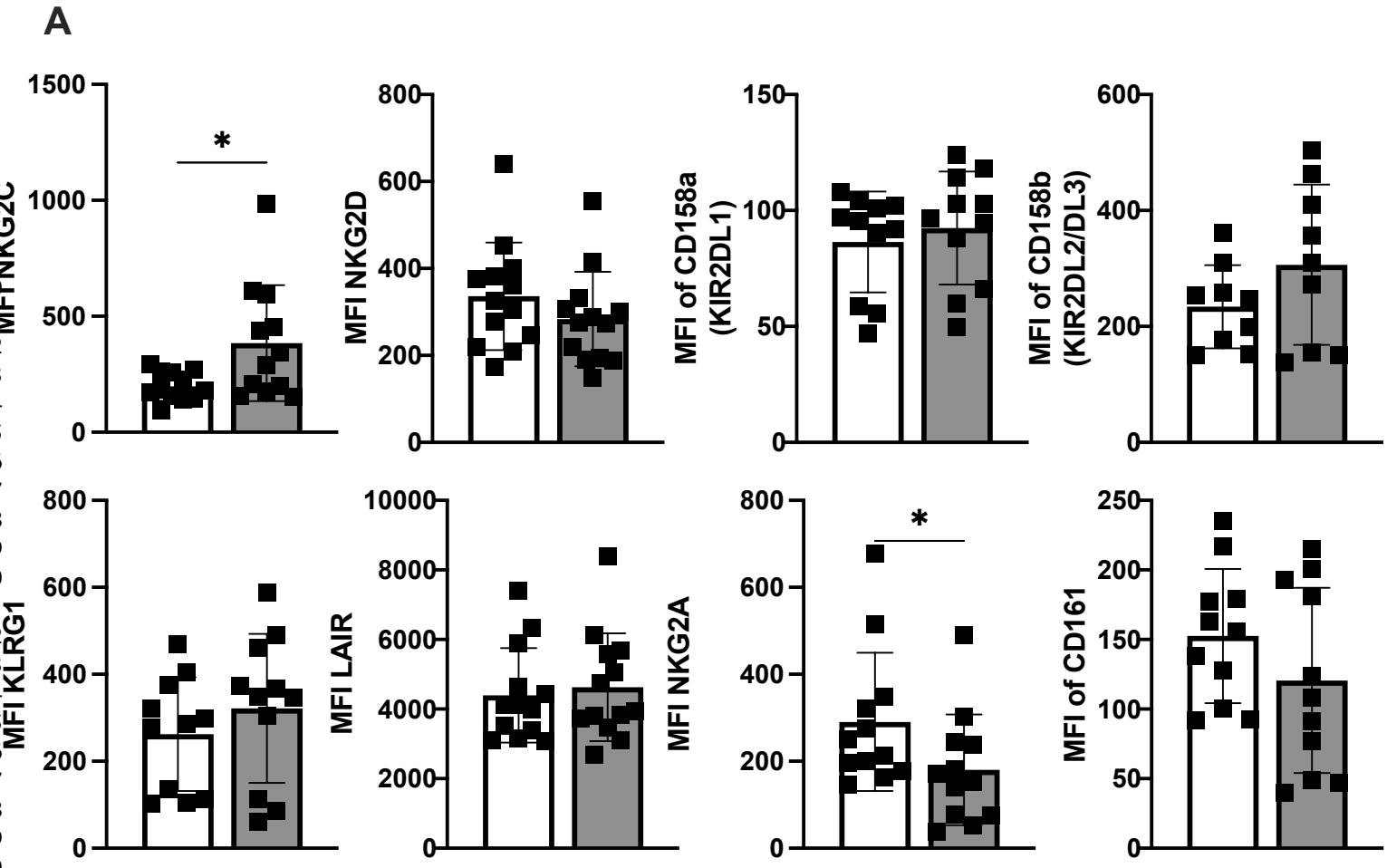
A
CD57-
CD57+
MFI NKG2C
1500
1000
500
0
*
MFI NKG2D
800
600
400
200
0
MFI of CD158a (KIR2DL1)
150
100
50
0
MFI of CD158b (KIR2DL2/DL3)
600
400
200
0
MFI KLRG1
800
600
400
200
0
MFI LAIR
10000
8000
6000
4000
2000
0
MFI NKG2A
800
600
400
200
0
*
MFI of CD161
250
200
150
100
50
0

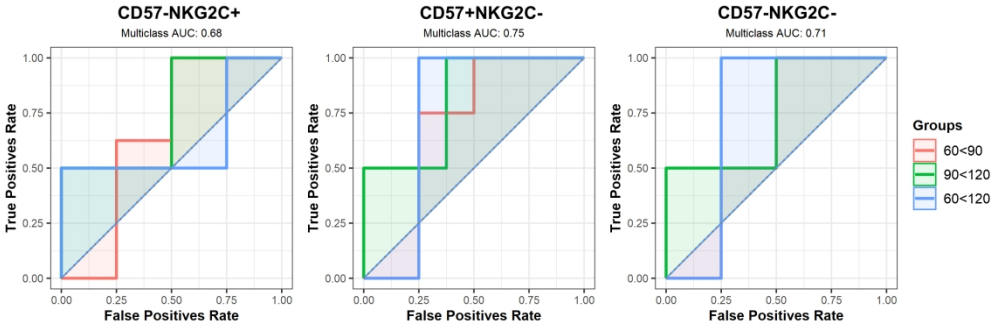

1058x352mm (72 x 72 DPI)

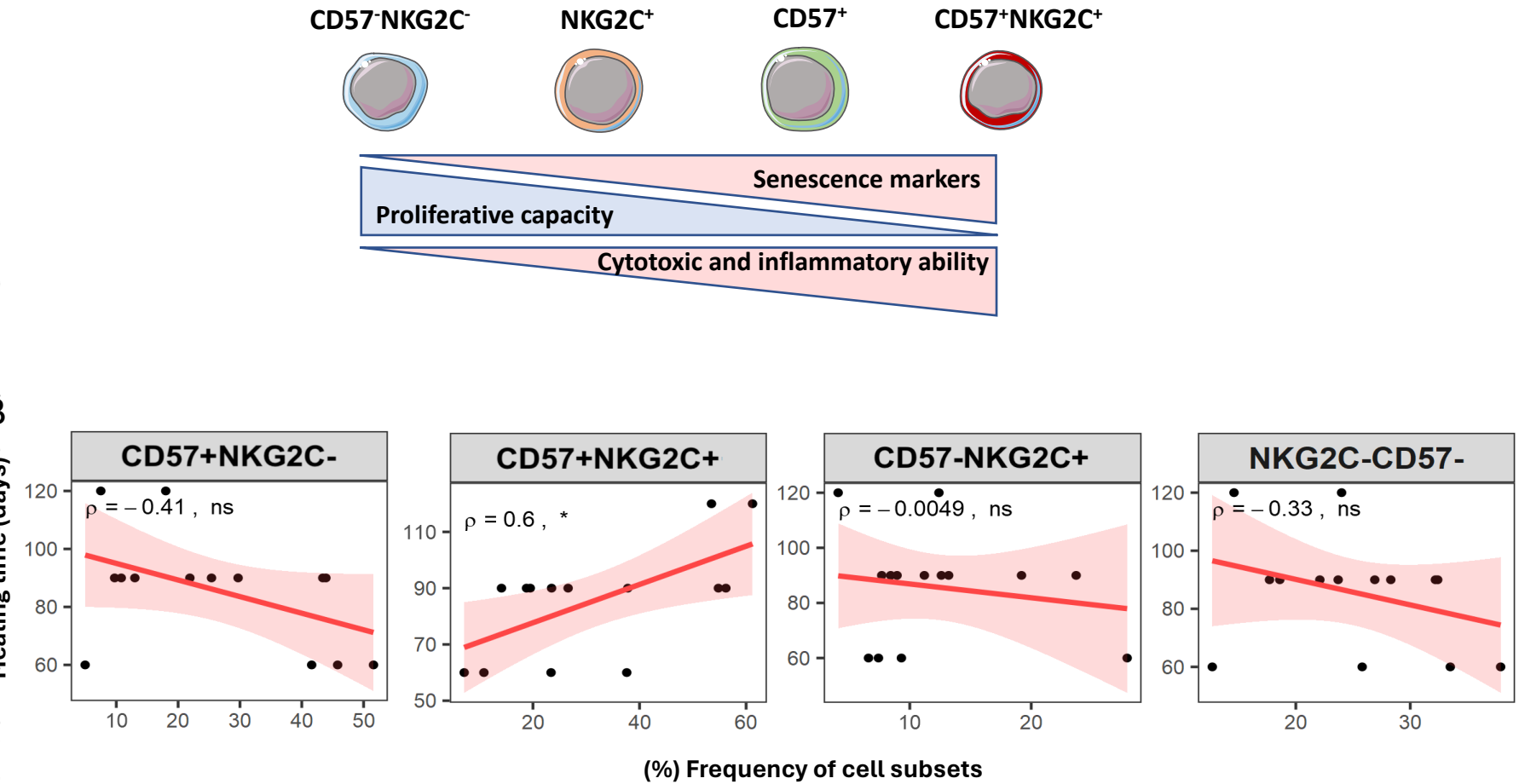
A
CD57-NKG2C-
NKG2C+
CD57+
CD57+NKG2C+
Senescence markers
Proliferative capacity
Cytotoxic and inflammatory ability
B
CD57+NKG2C-
CD57+NKG2C+
CD57-NKG2C+
NKG2C-CD57-
ρ = – 0.41 , ns
ρ = 0.6 , *
ρ = – 0.0049 , ns
ρ = – 0.33 , ns
Healing time (days)
(%) Frequency of cell subsets